A Compact Silicon-based Photonic Phase-tunable Microwave Frequency Downconverter

Xingyi Jiang[1], Qiang Zhang[2*], Shengyu Fang[1], Shuyue Zhang[1], Hui Yu[2]
[1]*College of Information Science and Electronic Engineering, Zhejiang University, Hangzhou 310027, China*
[2]*Zhejiang Lab, Hangzhou 311121, China*
**Corresponding author: zhangqiang@zhejianglab.com*

Abstract: We experimentally demonstrate a compact silicon-based photonic frequency downconverter with tunable phase shift. It can be operated at 20/40 GHz while supporting a 137° phase shift of 0.04 GHz IF signal. © 2023 The Author(s)
OCIS codes:(130.0130) Integrated optics; (060.5625) Radio frequency photonics

1. Introduction

Microwave frequency down-conversion is a key signal processing function that down-converts a radio frequency (RF) signal to an intermediate frequency (IF) for further detection and processing. Compared with the electronic downconverter, photonic downconverters have attracted more attention due to the advantages of large bandwidth, high flexibility and strong electro-magnetic interference immunity [1]. Many researchers have designed and optimized various photonic downconverters in several microwave system applications [2]. In microwave phased-array beamforming networks and phase-coded radar systems, the capability of broadband phase manipulation is demanded [3]. Recently, several schemes of photonic microwave frequency down-conversion with a broadband phase tunability are proposed [4]. It can be seen that, such systems are constructed by the discrete optical components, introducing larger volume, higher power consumption and higher cost. Recently, [5] demonstrates silicon-based photonic mixer subsystems based on Mach-Zehnder modulators (MZMs). However, it occupies large size and not support the tunable phase shift of the IF signal. Here, we design and demonstrate a more compact photonic phase-tunable microwave frequency downconverter circuit based on silicon photonics integration platform. The size of the component is merely 200×700 μm^2. It supports the frequency down-conversion at 20/40 GHz. Furthermore, the phase of measured IF signal with frequency of 0.4 GHz can be continuously altered from 0° to 137° with RF signal.

2. Device Architecture & Linearization Principle

The schematic diagram and the microscope image of our designed photonic microwave frequency downconverter circuit are shown in Figs. 1(a) and 1(b), respectively. The device is composed of two identical carrier-depletion-type micro-ring modulators (MRM-1 & MRM-2), two TiN-based heaters, a resonator-based optical bandpass filter (OBPF) and a germanium photodiode (Ge PD). The photonic circuit is fabricated on the silicon-on-insulator (SOI) wafer with a 220 nm thick silicon layer and a 3 μm thick buried oxide (BOX) in Singapore advanced micro foundry (AMF). The radius of the MRM is 10 μm while the gap between ring and bus waveguide is 200 nm.

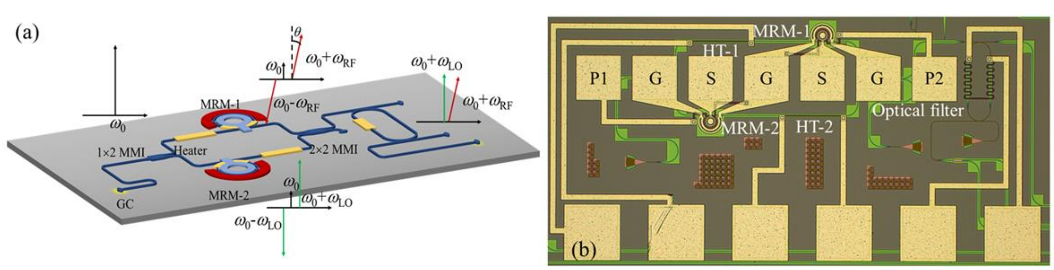

Fig. 1 (a) Schematic diagram of the proposed mixing system, GC, grating coupler; MMI, multi-mode interference; MRM, micro-ring modulator; PD, photodetector. (b) Optical microscope images of the silicon-based microwave frequency downconverter.

As shown in Fig. 1(a), an optical carrier from a continuous wave laser diode, $E(t)=E_0\exp(j\omega_0 t)$, is injected into the device and split into two MRMs by a 1×2 multimode interferometer (MMI). E_0 and ω_0 are the amplitude and angular frequency of optical carrier, respectively. The RF and local oscillator (LO) microwave signals are fed to the MRM-1 and MRM-2, respectively. Subsequently, such two microwave signals are transferred from electric domain to optical domain and combined by a 2×2 MMI. Using the OBPF to select the two optical upper sidebands with frequencies of $\omega_0+\omega_{RF}$ and $\omega_0+\omega_{LO}$, which are expressed as Eqs. (1) and (2),

$$E_{MRM1-RF-up}(t)=\sqrt{P_1}e^{j[(\omega_0+\omega_{RF})+\varphi_1]} \quad (1)$$

$$E_{MRM2-LO-up}(t)=\sqrt{P_2}e^{j[(\omega_0+\omega_{LO})+\varphi_2]} \quad (2)$$

Where $P_{1/2}$ means the optical power of the corresponding first-order upper sideband from MRM-1/2. ω_{RF} and ω_{LO} denote the angular frequencies of RF and LO signals, respectively. φ_1 and φ_2 are the phase of the corresponding optical sideband signals which can be controlled by thermal-optic phase shifters (TiN-based heaters). After sending the selected two optical signals into a high-speed photodetector, the detected photocurrent can be expressed as

$$i_{PD}=\frac{R}{2}(P_1+P_2)+R\sqrt{P_1P_2}\cos\left[(\omega_{RF}-\omega_{LO})t+(\varphi_1-\varphi_2)\right] \quad (3)$$

Here, R means the responsivity of the photodetector. In practical experiment, the bandwidth of employed photodiode is slightly larger than the IF signal for filtering the higher frequency term with frequency of $\omega_{RF}+\omega_{LO}$. It can be seen that, the frequency and phase of the generated IF signal, f_{IF} and θ, equal to ω_{RF}-ω_{LO} and φ_1-φ_2, respectively. Therefore, our proposed silicon photonic circuit can implement frequency down-conversion and phase shifting for RF signal simultaneously.

3. Experiments and Results

The experimental setup of the proposed photonic microwave frequency downconverter with tunable phase is illustrated in Fig. 2. A TE polarized lightwave, at a wavelength of 1550 nm and with output power of 13 dBm, from a continuous wave (CW) tunable laser (Santec TSL-710) is coupled into and out of the photonic integration circuit (PIC) by two fiber grating couplers (GCs). The optical carrier is split equally into the two carrier-depletion-type MRMs via a 1×2 MMI. The RF and LO microwave signals, with power of 25 dBm, are generated from two analog signal generators (Keysight E8267D). These two microwave sources are previously synchronized. The RF and LO signals are combined with two DC bias voltages (-2V) before being fed to the two MRMs by a 67 GHz PGSGSGP RF probe. The DC probes in the 7-claw probes are connected to DC voltages (supported by a control circuit) and applied to the DC pads (P1 & P2 in Fig. 1b) for tuning the operation wavelengths of MRMs. Here, the two MRMs are operated at the points with largest optical modulation amplitude (OMA).

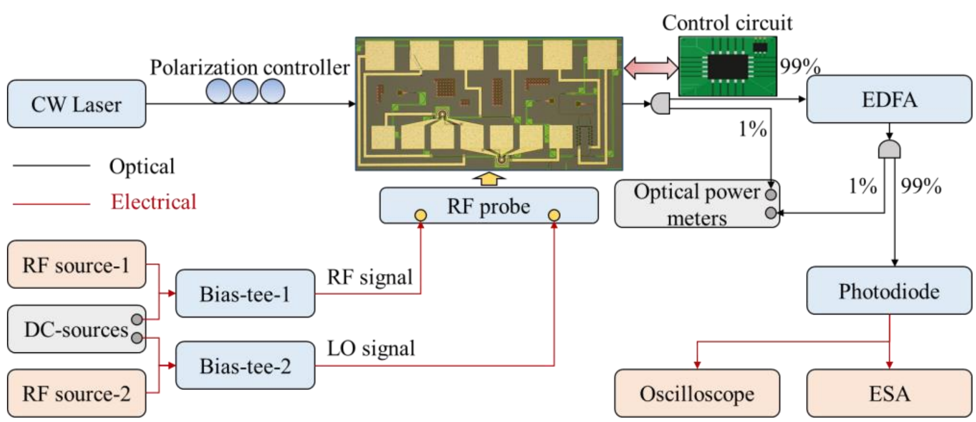

Fig. 2. Experimental setup of the proposed photonic frequency down-conversion with phase shift. CW: Continuous wave; EDFA: erbium-doped fiber amplifier; DC: direct current; RF: Radio frequency; LO: Local oscillator; ESA: Electrical signal analyzer.

Two modulated optical signals are mixed via a 2×2 MMI. Subsequently, two desirable optical sidebands with frequency of $\omega_0+\omega_{RF}$ and $\omega_0+\omega_{LO}$, are selected by the resonator-based OBPF. The output optical signal output from the PIC is amplified by an erbium doped amplifier (EDFA) so as to compensate the ~ 12 dB coupling loss of two fiber grating couplers and the insertion loss of the device itself. Two 1/99 optical power splitters are used to monitor the operation states of MRMs and the output optical power of EDFA. Finally, the detected electrical signal of the PD is fed to an electrical signal analyzer (ESA)/oscilloscope for study the spectrum information/phase of the IF signal. To increase the output power of IF signal while make the photodiode operated at linear region, the optical power injected to PD is set at 6 dBm. First, we choose the RF signals with the frequencies of 20.01 GHz and 40.01 GHz while choose the LO signals with the corresponding frequencies of 20 GHz and 40 GHz to investigate the down-conversion ability. As the spectrums are shown in Figs. 3(a) and (b), the converted IF signals with frequency of 0.01 GHz are observed by the ESA. Due to the limited modulation bandwidth of the two MRMs, the converted IF power in Fig. 3(b) is lower than that in Fig. 3(a).

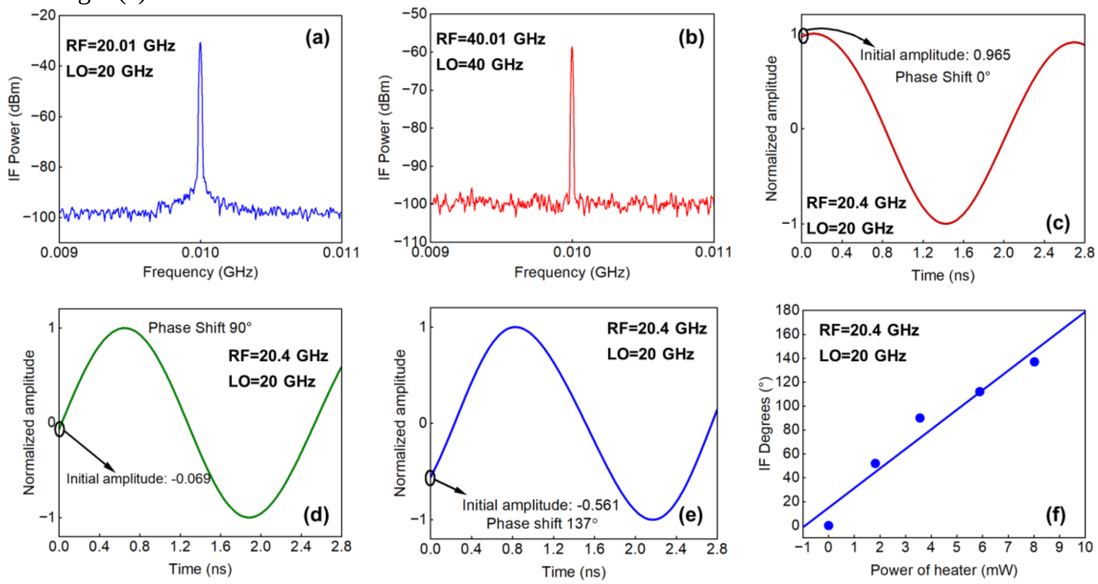

Fig. 3. The measured spectrums of down-converted IF signals (a) with RF and LO signals of 20.01GHz and 20 GHz, (b) with RF and LO signals of 40.01GHz and 40 GHz; Measured temporal waveforms of IF signals when RF and LO signals with frequencies of 20.04 GHz and 20 GHz while its phase shift is (c) 0°, (d) 90° and (e) 137°; (f) The relationship between the phase of IF signal and the heating power.

Subsequently, according to the theoretical analysis, the phase shift of the IF signal can be controlled by tuning the heating power of the heater (HT-1/2) that is shown in Fig. 1(b). Here, the RF and LO signals are set as frequencies of 20.04 GHz and 20 GHz, respectively. After altering the heating power to 0 mW, 3.56 mW and 8.02 mW, the phases of the corresponding detected IF signal are shifted to 0°, 90° and 137°, respectively. The corresponding measured temporal waveforms are shown in Figs. 3(c) to (e). Based on the measured results, the relationship between the phase of IF signal and the heating power is fitted as Fig. 3(f).

4. Conclusion

We demonstrate a compact photonic frequency down-conversion system with tunable phase shift. According to the experiment results, the RF frequency from 20.01 GHz to 40.01 GHz can be down-converted to 0.01 GHz. Besides, the phase of IF signal at 0.4 GHz can be tuned to 137° when the heating power is 8.02 mW. Based on the fitted data, the phase of IF signal can be altered 360° when the heating power is increased to ~ 20 mW. Furthermore, our photonic frequency down-converter employs the technology of silicon photonics integration, brings the features of low cost and small volume, which is expected to be used in the phase-array radar, high-speed signal processing systems.

Acknowledgement

The authors would like to thank Dr. Bing Wei, Training Platform of Information and Microelectronic Engineering in Polytechnic Institute of Zhejiang University.

References

[1]. Marpaung D, et al., “Integrated microwave photonics”, Nature photonics, **13**(2), 80-90(2019).
[2]. Tang Z, et al., “Photonics‐based microwave frequency mixing: methodology and applications”, Laser & Photonics Reviews, **14**(1), 1800350(2020).
[3]. Lin T, et al., “Microwave photonics time-delayed mixer”, Journal of Lightwave Technology, **39**(10), 3145-3153(2021).
[4]. T. Jiang et al. “Photonic downconversion with tunable wideband phase shift”, Opt. Letter, **41**, 2640–2643 (2016).
[5]. Bottenfield C G, et al., “High-performance fully integrated silicon photonic microwave mixer subsystems”, Journal of Lightwave Technology, **38**(19), 5536-5545(2020).